Limnol. Oceanogr., 46(1), 2001, 86–94

Light absorption and size scaling of light-limited metabolism in marine diatoms

Zoe Vanessa Finkel[1]
Department of Biology, Dalhousie University, Halifax, N.S. Canada B3H 4J1

Abstract

Previous studies have found that the size-scaling exponent of metabolic rates in unicellular algae often deviates from the exponent of −1/4 usually found for heterotrophs. This study confirms a significant linear relationship between log cell volume (μm^3) and log intrinsic growth rate (h^{-1}), carbon-normalized photosynthetic capacity and performance (h^{-1}), and carbon-normalized respiratory rate (h^{-1}) for eight marine centric diatoms under nutrient-saturated, light-limited conditions. The intrinsic growth rate and carbon-normalized respiratory rate have size-scaling exponents not significantly different from −1/4, whereas the carbon-specific photosynthetic rates deviate from −1/4. The size dependence of the optical absorption cross section (m^2 mg chlorophyll a^{-1}) due to the package effect provides a mechanistic model that explains the anomalous size scaling of the anabolic rates of unicellular phytoplankton.

From bacteria to large mammals, body size can predict metabolic rate:

$$M/C = aV^b, \tag{1}$$

where a is a group-specific constant and b is the size-scaling exponent of the relationship between the metabolic rate (M) normalized to biomass (e.g., C, carbon) and the size of the organism (e.g., cell volume V; notation summarized in Table 1). Related organisms can have similar values of a, but it is often quite variable (Chisholm 1992). In contrast, b is commonly −1/4 when the metabolic rate is normalized to body mass (Peters 1983). Since this paper focuses on carbon-normalized rates, this exponent will be referred to as the −1/4 rule. For cellular metabolism, the size-scaling exponent is referred to as the 3/4 law or Kleiber's rule.

Cullen et al. (1993) suggest that cell size should be included in descriptions of phytoplankton growth intended for biogeochemical models. Cell size has been used to predict sinking rates, nutrient acquisition, light absorption, primary production, and growth, respiratory, and photosynthetic rates in phytoplankton (Joint and Pomroy 1988; Agusti 1991; Kiørboe 1993; Tang 1995). Several studies suggest that the size-scaling exponent of metabolic rates in phytoplankton deviates from the −1/4 rule, complicating attempts to predict metabolic rates from knowledge of biomass profiles and size spectra (Taguchi 1976; Lewis 1989; Sommer 1989). Some of the variability in the size scaling of phytoplankton metabolism may be a response to environmental conditions. Banse (1976) predicted a change in the metabolic size-scaling exponent with a degradation in growth conditions, and Schlesinger et al. (1981) found an increase in the size-scaling exponent of the intrinsic growth rate of freshwater algae with decreasing light intensity.

Although many mechanisms have been suggested, the cause of size scaling of metabolic rates is unclear. Several hypotheses attribute the cause of size scaling of metabolic rates to morphological features and physiological processes not available to unicellular photoautotrophs (Kleiber 1961; McMahon 1973; Peters 1983). For example, West et al. (1997) present a fractal model of the −1/4 rule based on the branching of tubular transport mechanisms of the mammalian cardiovascular system that is clearly not applicable to the unicellular protozoa (Beuchat 1997). Banse (1976) suggests that the surface area to volume ratio may be responsible for the size scaling of metabolic rates in algae. As the volume of a cell of constant shape increases, the surface area to volume ratio decreases. This will alter rates of passive gas and nutrient diffusion per unit volume, resulting in a size-scaling exponent of −1/3, not the commonly accepted value of −1/4 (Hemmingsen 1960; Kleiber 1961). Neither the −1/4 nor −1/3 rule can account for the range of size-scaling exponents associated with phytoplankton metabolism.

Light absorption may be responsible for the anomalous size scaling of the metabolic rates of phytoplankton (Finkel and Irwin 2000). Unlike heterotrophs, autotrophs depend on the absorption of light to drive their metabolic processes. Light absorption is a nonlinear function of the composition and concentration of pigment and cell size (Morel and Bricaud 1981; Kirk 1994). The optical absorption cross-section of phytoplankton cells (m^2 mg chlorophyll a^{-1}) is given by

$$a^* = 3/2 a_s^* Q(\rho)/\rho, \tag{2}$$

where

$$Q(\rho) = 1 + \frac{2e^{-\rho}}{\rho} + 2\frac{e^{-\rho} - 1}{\rho^2} \tag{3}$$

and

$$\rho = a_s^* c_i d, \tag{4}$$

where a_s^* (m^2 mg Chl a^{-1}) is the chlorophyll-specific absorption of the photosynthetic pigments in solution, Q and ρ are dimensionless, c_i ($10^9 \times$ pg Chl a μm^{-3}) is the intracellular Chl a concentration, and d is cell diameter (m).

An increase in cell size and/or intracellular pigment con-

[1] Present address: Institute of Marine and Coastal Sciences, Rutgers University, New Brunswick, New Jersey, 08901 (finkel@imcs.rutgers.edu).

Acknowledgements

This work was supported by a Dalhousie graduate scholarship. I thank T. Platt, S. Sathyendranath, P. Kepkay, J. Jellett, B. Irwin, W. K. W. Li, V. Stuart, E. Head, V. Lutz, R. Campbell, J. Bugden, A. Irwin, P. Falkowski, O. Schofield, and two anonymous referees.

Table 1. List of symbols. The superscripts * and C refer to normalization of the parameter by mg Chl *a* or mg carbon.

Symbol	Description	Units
$\bar{a}$	Spectrally averaged absorption cross section	m^2
α	Photosynthetic efficiency	mg C h^{-1} μmol photons m^{-2} s^{-1}
C	Intracellular carbon content	μg
c_i	Intracellular Chl *a* concentration	pg Chl *a* μm^{-3}
Chl	Total intracellular Chl *a* content	pg
I	Available irradiance	μmol photons m^{-2} s^{-1}
I_k	P_{max}/α	μmol photons m^{-2} s^{-1}
μ	Intrinsic growth rate	h^{-1}
P_{max}	Photosynthetic capacity	mg C h^{-1}
P_k	Photosynthetic performance	mg C h^{-1}
ϕ_{PSII}	Quantum yield of photochemistry	Dimensionless
ϕ_μ	Quantum yield of growth	Dimensionless
ϕ_p	Quantum yield of photosynthesis	Dimensionless
^{14}CR	Respiration derived from PI curve	mg C h^{-1}
^{O}R	Respiration derived from oxygen consumption	mg C h^{-1}
θ	Carbon : Chl *a*	wt : wt
V	Cell volume	μm^3

centrations results in a decrease in a^*, reflected in a decrease in

$$Q^* = a^*/a_s^*, \quad (5)$$

referred to as the ''package effect'' (Morel and Bricaud 1981). Under the assumption of uniform c_i and that the $-1/4$ size scaling of metabolic rates reported in heterotrophs still occurs in autotrophs, steeper size scaling is expected for the anabolic rates of light-limited unicellular autotrophs (Finkel and Irwin 2000). The exact nature of the size scaling of the anabolic rates depends on the relationship between c_i and cell size. The general idea is that the package effect modifies the size scaling of light-limited metabolic rates by changing a^*, thereby altering the amount of energy available for the metabolic reactions.

This study addresses two questions. First, does the size-scaling exponent of the intrinsic growth rate, carbon-specific rate of photosynthesis, and respiration deviate from the $-1/4$ rule under suboptimal growth conditions, specifically subsaturating irradiance? Second, can the effect of pigment packaging on the light-absorptive properties of the cells explain anomalous size scaling in photosynthesis? To address these questions, photosynthesis, respiration, growth, the efficiencies of growth and photosynthesis, and light-absorptive properties were quantified for eight diatom species that range in size from ~10 to 250,000 μm^3.

Materials and methods

Phytoplankton cultures and growth conditions—Eight centric diatom species were chosen, representing a wide spectrum of cell sizes: *Chaetoceros calcitrans* (CCMP1315), *Thalassiosira (*or *Cyclotella) pseudonana* (CCMP1335), *Chaetoceros* sp. (no official identification), *Thalassiosira weissflogii* (CCMP1336), *Hyalodiscus* sp. (CCMP1679), *Planktoniella sol* (CCMP1608), *Coscinodiscus* sp. (CCMP312), and *Coscinodiscus* sp. (CCMP1583). All species had numerous discoid chloroplasts, except for the *Chaetoceros* spp. which have one or more sheet-like plastids (Round et al. 1990). All cultures were obtained from the Provasoli-Guillard National Center for the Culture of Marine Phytoplankton (CCMP), with the exception of *Chaetoceros* sp., which were isolated from the Huntsman Marine Science Center in St. Andrews, New Brunswick (J. Jellett pers. comm.). Cultures were grown in 2.8-liter glass Fernbach flasks at 20°C in *f*/2-enriched, 0.45-μm filtered Bedford Basin seawater (Guillard and Ryther 1962). The cultures were illuminated by a combination of broad-spectrum Sylvania fluorescent tubes F30T12 and F15T12D to a continuous photon flux density of 25 μmol photon m^{-2} s^{-1}, as measured by a biospherical light sensor placed in the culture vessel filled with media. Cultures were manually agitated approximately once per day.

Semicontinuous culture technique (Ukeles 1973) kept the cultures in exponential growth for a minimum of three generations prior to the photosynthetic experiments. The exponential growth rate was considered reached once the growth rate no longer increased with an increased rate of influx of new culture media. To minimize bacterial contamination, careful aseptic technique was used in the maintenance and growth of all cultures.

Estimates of phytoplankton biomass—The diameter (d) and height (h) of the diatoms were measured under the microscope with an ocular ruler. For each species, between 80 and 100 measurements were made of each dimension. The average cell volume was calculated from the average cell height and average square radius, under the assumption that all cells were cylinders. Two sets of cell size measurements were combined to derive an average estimate of cell volume associated with the growth rate. *Hyalodiscus* sp. doublets were treated as single cells because doublets were surrounded by a thick mucilaginous coating.

Chl *a* concentrations were determined fluorometrically, in triplicate, from samples concentrated on filters and then extracted for ≥24 h in ice-cold 90% acetone (Holm-Hansen et al. 1965). In addition, high-performance liquid chromatog-

raphy (HPLC) analysis provided estimates of the concentration of chlorophylls, carotenoids, and other accessory pigments in a subset of the samples. Samples were run on a Beckman C18, reversed phase, 3-mm Ultrasphere column by use of the solvent gradient system of Head and Horne (1993). Fluorometer estimates were calibrated with HPLC determinations of Chl *a*. Carbon content was determined with a Perkin-Elmer 2400-CHN Elemental Analyzer. Phytoplankton were filtered onto precombusted GF/F filters and placed in the freezer or desiccator until analysis.

The number of cells per unit volume for the five smallest diatoms was determined by use of the Levy Improved Neubauer and American Optical Brightline haemacytometers (both 0.2 mm deep). For each cell density estimate a minimum of four slides were counted. The cell densities of the three larger clones were determined by use of a Sedwick-Rafter chamber that was divided into 11 fields of view. Generally, two to four chambers were examined. When practical, enough cells were counted to keep the coefficient of variation of the mean population estimate <20%. The $\log_e$ growth rate (μ in h^{-1}) was determined by use of linear regression, as described by Guillard (1973).

Photosynthesis-irradiance (PI) experiments—Photosynthetic rate was estimated with $NaH^{14}CO_3$, following the method of Irwin et al. (1986), with some modifications. Each experiment employed 30 light bottles and 3 dark bottles, which were filtered after a 1-h incubation at the experimental irradiance. Inorganic carbon was removed by placing the filters over concentrated HCl for 20–30 min prior to placement in scintillation fluid. Disintegration per minute, measured by a Beckman LS 5000-CE liquid scintillation counter, were converted to photosynthetic rates, as described by Geider and Osborne (1992). A three-parameter hyperbolic tangent function was fitted to the PI data:

$$P(I) = P_{\max}\tanh(\alpha I/P_{\max}) - {}^{14}CR, \tag{6}$$

where I is the irradiance in μmol quanta m^{-2} s^{-1}, $P_{\max}$ is the photosynthetic capacity in mg C h^{-1}, α is the photosynthetic efficiency in mg C h^{-1} μmol quanta m^{-2} s^{-1}, and ${}^{14}CR$ represents the dark respiratory rate in mg C h^{-1} (Platt and Jassby 1976). The ratio $P_{\max}/\alpha = I_k$ was calculated to determine the irradiance at which photosynthetic capacity is reached. In all cases, I_k was higher than the growth irradiance, verifying that all experimental species experienced light limitation.

Oxygen consumption—Changes in oxygen concentration were determined in the dark by an ENDECO oxygen electrode system calibrated with a series of Winkler titrations, following the method of Levy et al. (1977) and Kepkay et al. (1997). Electrodes were pulsed every 5 min over a 24–30-h period in a 1-liter jacketed glass vessel held at 20°C. The rate of oxygen consumption changed over the course of the incubation. Because of a variable rate of oxygen consumption over the first several hours, the rate of oxygen consumption over the last 14 h of the incubation is presented. A respiratory quotient of one was used to convert moles O_2 (moles C h)$^{-1}$ to h^{-1} (Blasco et al. 1982).

Phytoplankton absorption measurements—The ratio of incident irradiance to transmitted irradiance (the optical density) was obtained from a Shimadzu UV-2101 PC spectrophotometer equipped with an integrating sphere. Phytoplankton cultures were filtered under low pressure onto GF/F filters. The same volume of filtrate was filtered under low pressure onto a second GF/F filter. The two filters were placed in the spectrophotometer in special filter holders, with the filtrate collected on the second filter serving as a blank. The absorption of the phytoplankton culture and detritus was estimated by use of the methods described in Hoepffner and Sathyendranath (1993) and references therein. A correction factor was applied to the optical densities determined from the filters. The correction factor (path-length amplification or β-factor) was determined by fitting a two-parameter quadratic function to the experimentally determined optical density data from filters and in suspension, as described by Mitchell (1990). Spectrally averaged absorption ($\bar{a}$) was calculated by integrating the absorption over all measured wavelengths and dividing by the number of wavelengths measured

$$\bar{a} = \frac{\int_{400}^{700} a(\lambda)\, d(\lambda)}{\int_{400}^{700} d(\lambda)}. \tag{7}$$

Quantum yield—The quantum yield of photochemistry (ϕ_{PSII}) was estimated from the measurement of in vivo dark-adapted fluorescence (F_0) and 3-[3,4-dichlorophenyl]-1,1-dimethyl urea–enhanced fluorescence (F_m), following the method of Geider et al. (1993), where

$$\phi_{\text{PSII}} = \frac{F_m - F_0}{F_m}. \tag{8}$$

The quantum yield of carbon fixation (ϕ_p) is calculated by

$$\phi_p = 0.231\alpha/\bar{a}, \tag{9}$$

where 0.231 converts milligrams of carbon to moles, hours to seconds, and micromoles of quanta to moles of quanta (Platt and Jassby 1976). Note that ϕ_p may overestimate the true value, because α may provide an estimate closer to gross than net photosynthesis. The effect of the spectral quality of the tungsten light on photosynthetic efficiency was corrected according to the method of Kyewalyanga (1997).

At the growth irradiance, the quantum yield of growth (ϕ_μ), was calculated following a simplified form of the equation provided by Sosik and Mitchell (1991):

$$\phi_\mu = 4.32 \times 10^7 \frac{\mu\theta}{aI}, \tag{10}$$

where μ is the growth rate (h^{-1}), θ is the C:Chl *a* ratio (mg:mg), a^* is the Chl *a*–specific absorption coefficient in m^2 mg Chl a^{-1}, I is the irradiance in the growth incubator in μmoles m^{-2} s^{-1}, and 4.32×10^7 is the product of 12,000, which is a constant that converts milligrams of carbon into moles of carbon, and 3600, which converts the growth rate from s^{-1} to h^{-1}. The quantum yield was corrected to account

Table 2. OLS and RMA regression coefficients associated with the relationship between the log of the cellular components, metabolic and physiological parameters, and log cell volume. Symbols are as defined in Table 1.

Equation	n	OLS regression coefficients		RMA regression coefficients		r^2
		Intercept (±SE)	Slope (±SE)	Intercept (±SE)	Slope (±SE)	
Chl	16	−1.678 ± 0.135	0.690 ± 0.036	−1.707 ± 0.083	0.699 ± 0.035	0.96
C	8	−6.864 ± 0.146	0.963 ± 0.060	−6.816 ± 0.253	0.949 ± 0.069	0.97
θ	8	1.055 ± 0.119	0.193 ± 0.049	1.065 ± 0.204	0.189 ± 0.056	0.66
c_i	16	−1.678 ± 0.136	−0.310 ± 0.035	−1.659 ± 0.083	−0.313 ± 0.035	0.84
P^{C}_{max}	24	−0.168 ± 0.170	−0.440 ± 0.046	−0.108 ± 0.108	−0.457 ± 0.046	0.81
P^{C}_{k}	24	−0.153 ± 0.177	−0.453 ± 0.048	−0.087 ± 0.113	−0.473 ± 0.048	0.80
$^{14C}R^{C}$	22	−2.080 ± 0.112	−0.284 ± 0.030	−2.070 ± 0.069	−0.288 ± 0.029	0.82
$^{O}R^{C}$	24	−1.352 ± 0.292	−0.290 ± 0.077	−1.216 ± 0.195	−0.329 ± 0.084	0.39
μ	8	−1.172 ± 0.113	−0.220 ± 0.030	−1.168 ± 0.064	−0.221 ± 0.026	0.90
$\bar{a}^{*}$	7	−1.585 ± 0.030	−0.077 ± 0.012	−1.585 ± 0.052	−0.077 ± 0.014	0.85
$\bar{a}^{C}$	7	−2.476 ± 0.137	−0.359 ± 0.056	−2.500 ± 0.233	−0.352 ± 0.065	0.85
ϕ_p	7	−1.045 ± 0.075	−0.138 ± 0.031	−1.048 ± 0.129	−0.137 ± 0.036	0.74

for variation in the spectrum of the fluorescent lights in the growth chamber, as described above for the tungsten lamp. Spectral irradiance values for the fluorescent tubes were provided by Sylvania.

Regression analysis and the determination of size-scaling exponents—According to the allometric power law (Eq. 1), metabolic rates can be described by an expression relating cell size to an exponent. Least-squares regression analysis (OLS) and reduced major axis regression (RMA) were both performed to determine the size-scaling exponent and intercept. According to Ricker (1973) and LaBarbera (1989), RMA is preferable to OLS, although results will converge as the correlation coefficient increases. The RMA regression minimizes the squared normal deviates, following the method of Kermack and Haldane (1950) and York (1966). OLS regression parameters are more commonly reported than RMA regression parameters. For consistency, only the OLS regression coefficients are referred to in the text. Regression coefficients will be referred to as statistically significant at the 95% significance level, and means are reported with their standard errors.

Results

Cell size and cellular composition—The eight species in this study span an ~250,000-fold range in volume, from just over 10 to over 250,000 μm^3. All species have similar pigment composition. Chl *a* and fucoxanthin represent 70%–89% of the total cellular pigment content. Chl *c*, β-carotene, and diadinoxanthin account for the majority of the remaining pigment. Pigment and carbon content per cell had positive, statistically significant relationships with cell volume (Table 2). Intracellular carbon appears to be approximately linearly related to cell volume. In contrast, intracellular Chl *a* content has a size-scaling exponent of 0.69 ± 0.04, resulting in an increase in the carbon : Chl *a* ratio (θ) with cell volume. The increase in θ results in systematically larger size-scaling exponents associated with the Chl *a* versus the carbon-normalized metabolic and physiological rates. The subsequent allometric analyses focus on the carbon-normalized rates, indicated by a superscript C.

The size scaling of metabolic processes—The size-scaling exponents associated with the cellular composition, metabolic rates, and physiological parameters of the marine diatoms are presented in Table 2. The intrinsic growth rates μ of the diatom clones span a 7.8-fold range, with doubling times from 33 h for the smallest clone to 258 h for the second-largest clone. The size-scaling exponent of μ is −0.22 ± 0.03, which is not significantly different from the −1/4 rule (Fig. 1*A*).

The carbon-specific respiratory rates, $^{14C}R^{C}$ and $^{O}R^{C}$, decrease similarly to μ with cell volume (Fig. 1*B*). Oxygen electrode estimates of respiration are, on average, approximately an order of magnitude higher than the ^{14}C estimates, but the size scaling of oxygen consumption supports and reinforces the size dependence found for the ^{14}C estimates of respiratory loss. Note that the average $^{14C}R^{C}$ for *T. pseudonana* was negative, and therefore was excluded from the analysis.

In contrast to μ and R^{C}, the size scaling of P^{C}_{max} and P^{C}_{k} significantly differ from the −1/4 rule (Fig. 1*C*). Carbon-specific photosynthetic capacity (P_{max}) and photosynthetic performance (P_k) have size-scaling exponents significantly less than those associated with growth and respiratory processes.

Phytoplankton absorption parameters—The absorption spectra of the diatom clones cluster in two distinct groups (Fig. 2*A*). *C. calcitrans*, *T. pseudonana*, and *Chaetoceros* sp., the three smallest species examined, have high $\bar{a}^{*}$ and high ratios of blue to red absorption. The four larger diatoms: *Coscinodiscus* spp, *Hyalodiscus* sp., and *T. weissflogii* have lower values of $\bar{a}^{*}$ and lower ratios of blue to red absorption. *P. sol* has a much higher $\bar{a}^{*}$, compared with other diatoms of comparable size, likely because of its large mucilaginous wing, and was therefore excluded from the analysis. The patterns of the Chl *a*–specific absorption spectra and spectrally averaged optical absorption cross sections

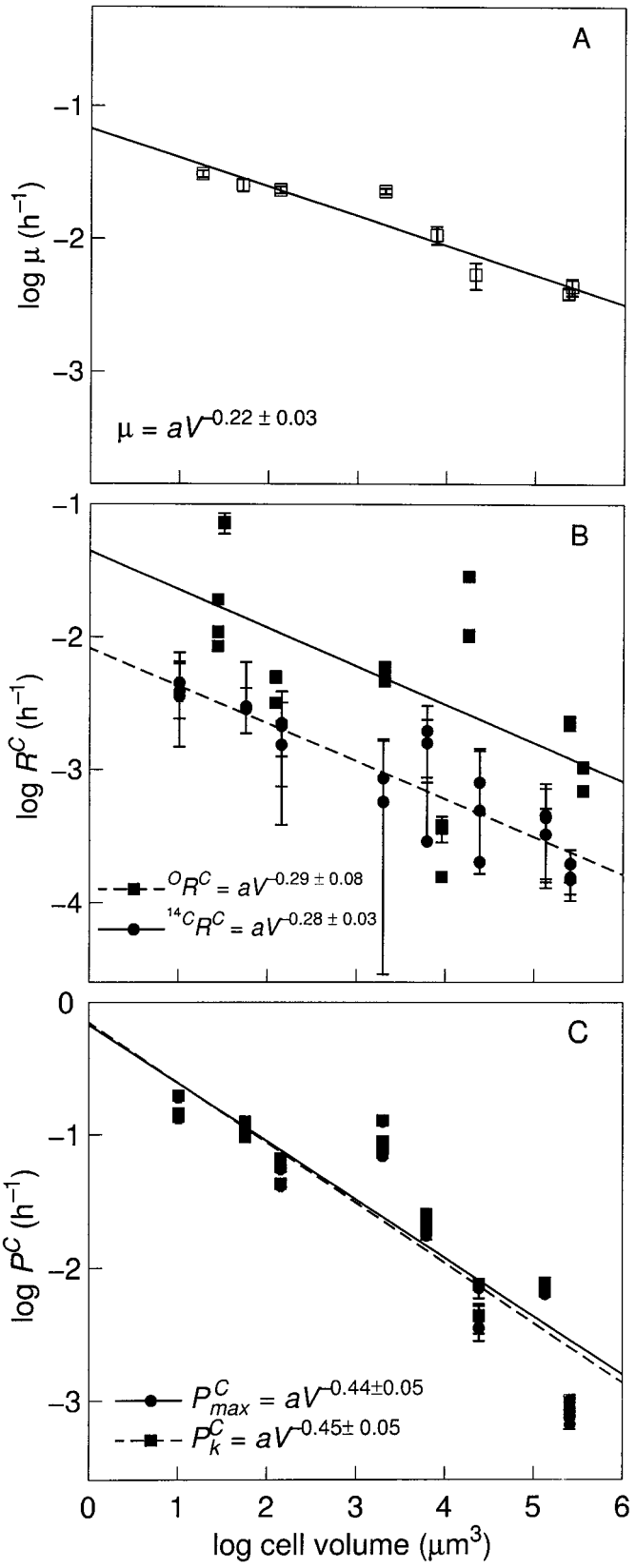

Fig. 1. Size scaling of growth, respiration, and photosynthesis with standard error bars and OLS lines. Standard error (SE) was not included for volume, because, in most cases, the error is smaller than the data point. (*A*) Instantaneous growth rate (μ; pm SE) at the growth irradiance. (*B*) Carbon-specific respiration: $^{14}C R^C$ is the indirect estimate of respiration from the PI curve, and $^{O}R^C$ is the oxygen estimate of respiration. (*C*) Carbon-specific photosynthesis: P^C_{max} is the photosynthetic capacity, and P^C_k is the photosynthetic performance.

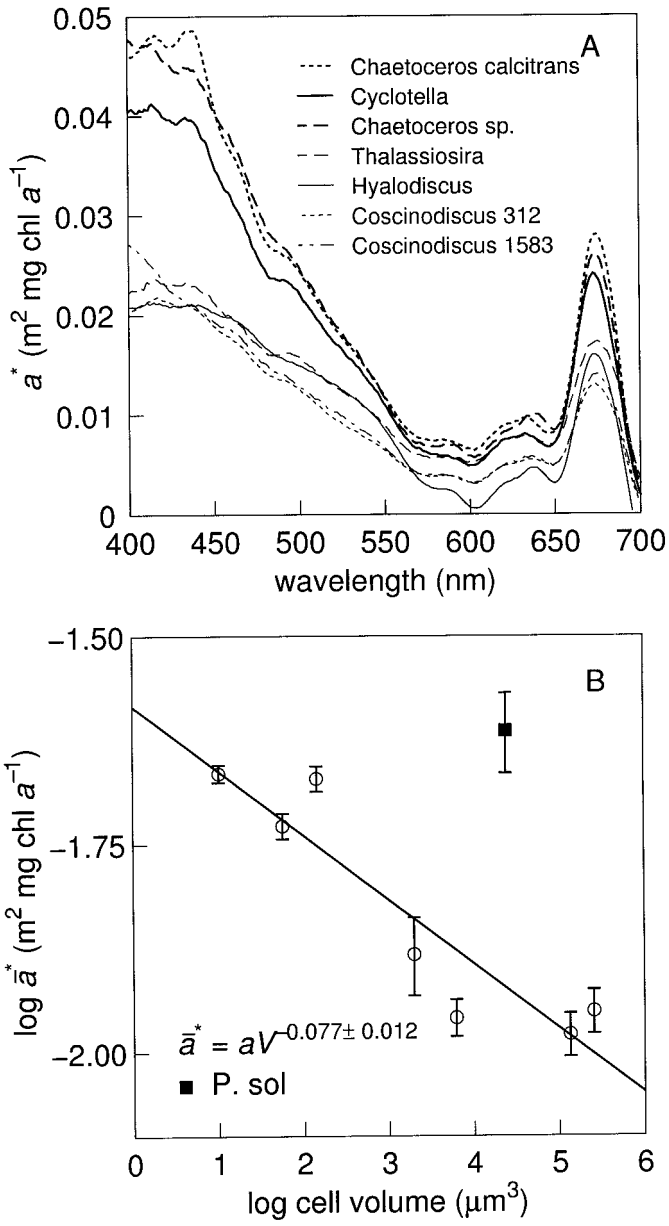

Fig. 2. Size dependence of light absorption. (*A*) Chl *a*–specific absorption spectra. *P. sol* is not shown. (*B*) Size dependence of the average Chl *a*–specific absorption coefficient ($\bar{a}^*$). The outlier *P. sol* is shown as a filled box. Error bars represent one SE.

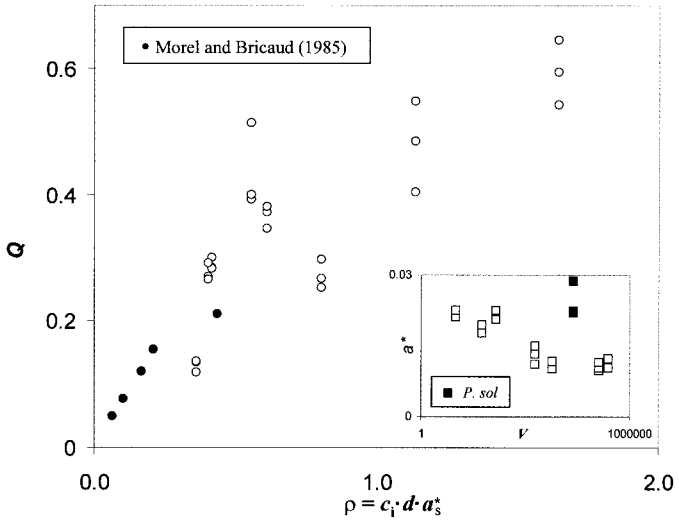

Fig. 3. Q at $\lambda = 676$ nm as a function of $\rho = c_i d a_s^*$. Five data points are included from Table 1 in Morel and Bricaud (1986): *Skeletonema costatum, Chaetoceros curvisetum, C. lauderi,* and *C. protuberans* (2 data points). Inset: Optical absorption cross section (m^2 mg Chl a^{-1}) at $\lambda = 676$ nm as a function of log cell volume (μm^3).

with cell volume (Fig. 2*B*) are consistent with an increase in the package effect with cell size.

Pigment composition, pigment concentration, and cell size can alter the optical absorption cross-section through the package effect. Pigment composition is very similar between the different diatom species. Considered separately, neither c_i nor cell size have a significant correlation with Q or the package effect. As predicted by Mie theory, Q, calculated at 676 nm to reduce the effect of pigments other than Chl *a*, increases concave down with $\rho = a_s^* c_i d$. Note that a_s^* is estimated as the specific absorption coefficient of Chl *a* extracted in acetone at the red peak (see Morel and Bricaud 1986). It is the combination of cell size and pigment concentration that control the efficiency factor for absorption (Q) and the approximate twofold decrease in the optical absorption cross section (Fig. 3).

The photosynthetic parameters, P^C_{max} and P^C_k are highly correlated with the spectrally averaged optical absorption cross section (Fig. 4*A*). Light-limited P_k is the product of the incident irradiance, $\bar{a}$, and the maximum quantum yield of photosynthesis. The effect of size-dependent $\bar{a}^C$ on the size-scaling exponent of light-limited P^C_k can be predicted by incorporating the $-1/4$ size scaling of metabolism into the bio-optic model of photosynthesis (Finkel and Irwin 2000). This can be done by decomposing ϕ_{max} into $\alpha^C/\bar{a}^C$ and constructing a hybrid α^C_{AB} that includes the biophysical processes that contribute to photosynthesis and the $-1/4$ size scaling of metabolism. For example, α^C_{AB} could be expressed as $\alpha^C_A \times \alpha^C_B$, where $\alpha^C_B = \phi_{max} \times \bar{a}^C$ incorporates the biophysics of light absorption and photosynthesis (Eqs. 2–4) and α^C_A introduces the $-1/4$ size scaling of metabolic rates (Eq. 1). The product α^C_{AB} is only one of many expressions that could be used to include the size scaling of metabolism into a bio-optical description of photosynthesis. A direct comparison of the predictions from this combined allometric–bio-optic

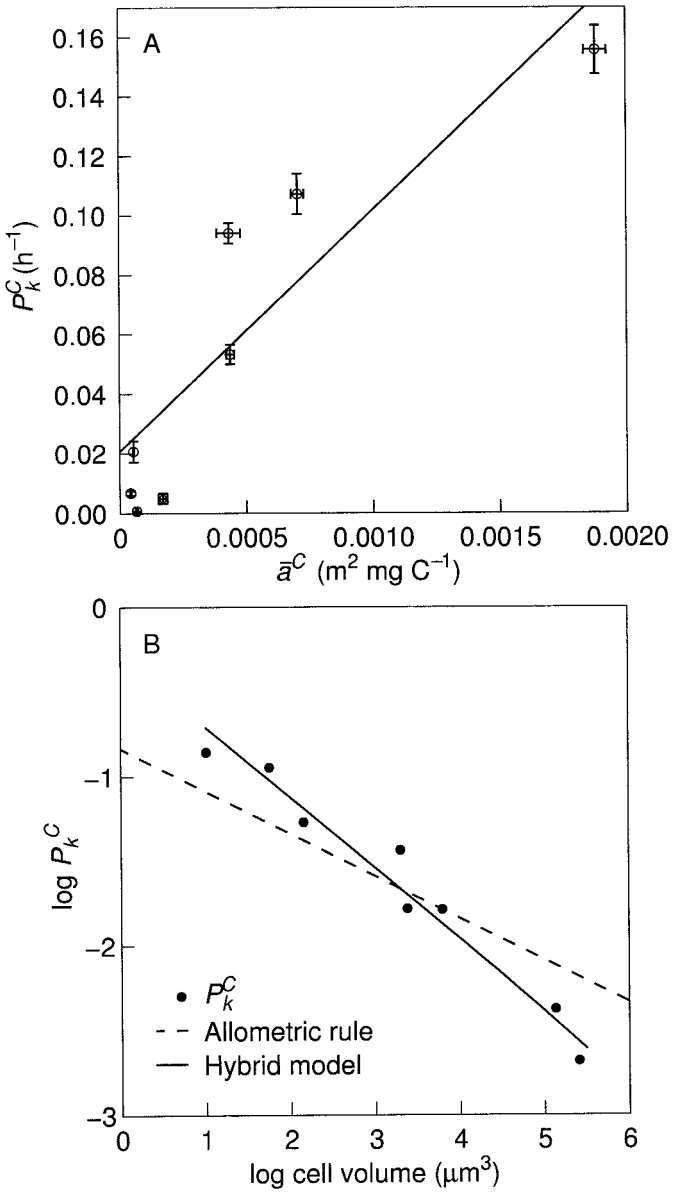

Fig. 4. Influence of the optical absorption cross section on photosynthesis. (*A*) Photosynthesis-absorption relationship: photosynthetic performance (P^C_k) as a function of the carbon-specific optical absorption cross section ($\bar{a}^*$). Error bars represent 1 SE. (*B*) Prediction of carbon-specific photosynthesis using a combination of the $-1/4$ rule and the size dependence of light absorption due to the package effect. Also shown is the $-1/4$ allometric rule and experimental data, P^C_k. Figure redrawn from Finkel and Irwin (2000).

model and P^C_k is provided in Fig. 4*B*. The agreement between the model (solid line) and the data (filled circles) is qualitatively superior to the simple $-1/4$ rule (dashed line). There is a shallower slope for small cells, and the curve is slightly concave down, reflecting the changing package effect with increasing cell size.

The efficiency of photosynthesis and growth—Three different estimates of quantum yield show different degrees of size dependence. The maximum quantum yield of photo-

chemistry, ϕ_{PSII}, is independent of cell size and is close to maximum reported values with a mean of 0.637 (Fig. 5*A*). In contrast, the quantum yield of photosynthesis (ϕ_p) is significantly lower than reported maximum values, ranging from 0.014 to 0.070 moles of carbon produced per mole of photons absorbed (a fivefold range), and has a statistically significant negative relationship with cell volume (Fig. 5*B*). Similar to ϕ_p, the quantum yield of growth (ϕ_μ) has a 4.5-fold range in values, from 0.02 to 0.09, but, in contrast to ϕ_p, ϕ_μ is not size dependent (Fig. 5*C*).

Discussion

This study confirms the significant linear relationship between log cell volume (μm^3) and log of the metabolic rates of the marine centric diatoms under nutrient-saturated, light-limited conditions. The intrinsic growth rate and carbon-normalized respiratory rate have size-scaling exponents not significantly different from $-1/4$, in agreement with Tang (1995) and Tang and Peters (1995). In contrast, carbon-specific P_k and P_{max} deviate from the $-1/4$ rule, in agreement with Taguchi (1976). These size-scaling coefficients are significantly less than $-1/4$, contrary to the suggestion made by Banse (1976) that the size-scaling exponent increases with suboptimal growth conditions.

Decreases in the optical absorption crosssection with cell size can explain the anomalously steep size-scaling exponent associated with light-limited photosynthetic performance. The diatom cells in this study exhibited a size-dependent decrease in $\bar{a}^*$ due to the increased self-shading of pigments (decrease in Q^*) within the cell with increasing cell volume (Morel and Bricaud 1981; Kirk 1994). The decrease in Q^* and thus $\bar{a}^*$ results in a decrease in P_k^C with cell size under subsaturating light intensities. An allometric–bio-optic model that combines the effect of size scaling in $\bar{a}^*$ due to the package effect with the $-1/4$ size scaling of metabolism can predict the observed anomalously low size-scaling exponent associated with P_k^C (Finkel and Irwin 2000). This prediction assumes that ϕ_{max}, pigment composition, and pigment concentration are independent of cell size.

In general, this study and previous evidence indicate that the quantum yield of photosynthesis and growth are independent of size (Geider et al. 1986). The quantum yield of photosynthesis or carbon assimilation (ϕ_p) provides an estimate of the efficiency of conversion of absorbed light energy into carbon products under low light. Theoretically, algae grown under low light and high nutrient concentrations should have a constant ϕ_p, close to the theoretical maximum (ϕ_{max}) between 0.1 and 0.125 (Geider et al. 1986; Kirk 1994). In the present study, ϕ_{PSII} and ϕ_μ are independent of cell size, but ϕ_p is variable and tends to decrease with increasing cell size. The size scaling of ϕ_p may be an artefact due to the method of measurement. The incorporation of ^{14}C can provide an ambiguous estimate of photosynthesis somewhere between net and gross photosynthesis, depending on the ratio of the experimental incubation to generation time of the organism (Li and Goldman 1981). Even given the size scaling of ϕ_p, the lack of size scaling associated with the quantum yield of growth and photochemistry supports the

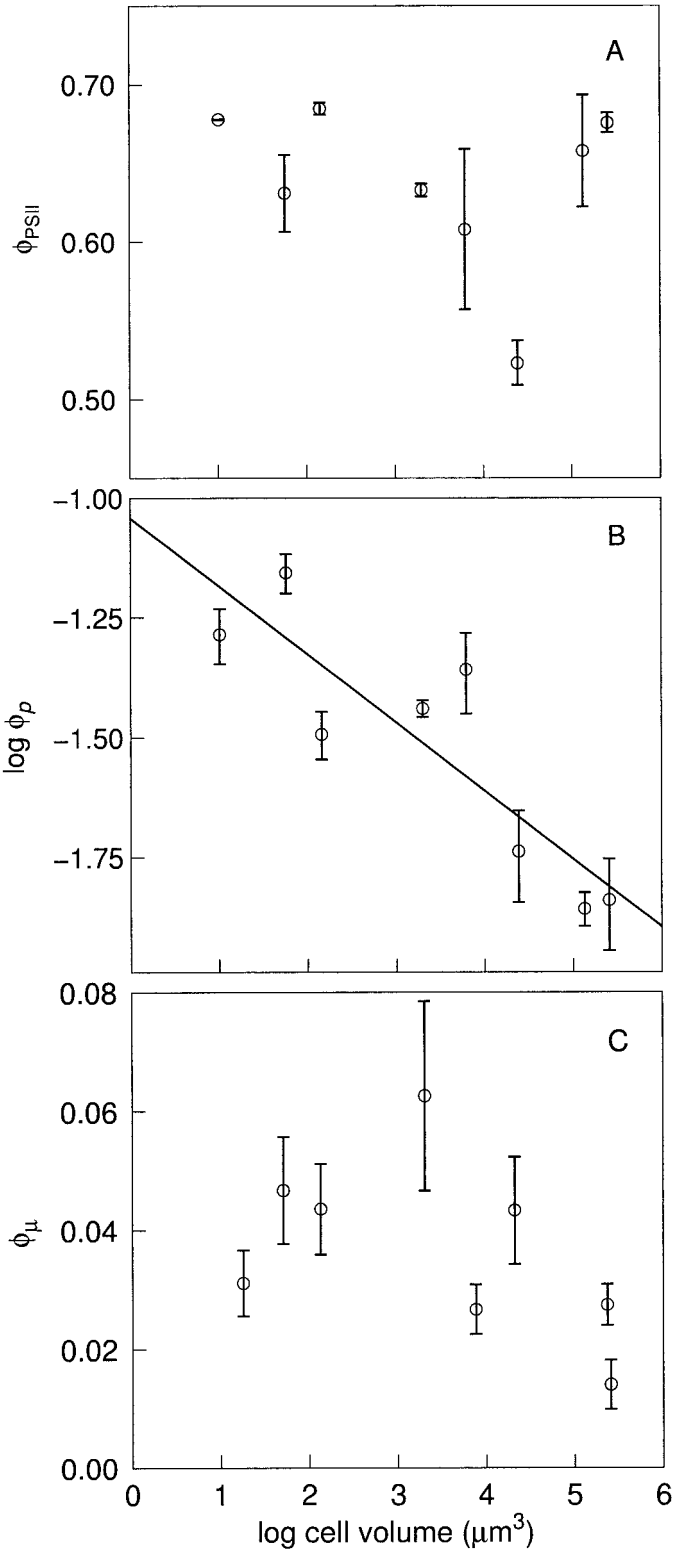

Fig. 5. Quantum yield of photosynthesis and growth with standard error bars. (*A*) Quantum yield of photochemistry (ϕ_{PSII}), (*B*) size dependence of the quantum yield of photosynthesis (ϕ_p), and (*C*) quantum yield of growth (ϕ_μ).

assumption of a constant ϕ_{max} and previous evidence that energetic efficiencies are independent of an organism's size (Peters 1983).

The diatom cells all have very similar pigment composition, leaving pigment concentration and cell size responsible for the variation in the optical absorption cross section. The intracellular Chl *a* concentrations (c_i) of the diatoms tend to decrease with cell volume. The decrease in c_i with cell size is common to many phytoplankton representing many different taxonomic classes (Agusti 1991). In comparison with constant c_i, the inverse relationship results in a moderation in the increase in the package effect with cell size (Finkel and Irwin 2000). This pattern suggests that selection may act on intracellular pigment concentration to optimize the fitness of the algal cell through the optical absorption cross section. Despite the decrease in c_i with cell size, there is still a slight increase in the package effect and a resulting decrease in $\bar{a}^*$ in the light-limited diatoms.

The increase in the package effect with cell size may result in the size scaling of the number of photosynthetic units n (O_2/Chl *a*). This is because at the same c_i, the probability that each Chl *a* molecule will intercept and absorb an incident photon decreases with cell size. The average decrease in photon capture by the individual pigment molecules with the package effect should set a practical upper limit on the number of photosynthetic units per cell of a given size. Analogously, Sukenik et al. (1990) found that n decreases when *D. tertiolecta* is transferred from a high to low light environment. It is not unreasonable to suggest that larger cells, like the cells exposed to lower irradiance, will experience a more acute package effect and have lower values of n than the smaller cells, which intercept relatively more of the incident irradiance per molecule of Chl *a*.

The size scaling of the number of photosynthetic units can explain the anomalous size scaling of both P_k and P_{max} under light-limiting conditions. Unlike P_k^C, P_{max}^C does not depend directly on the optical absorption cross section (Falkowski 1981). Following the notation described in Falkowski and Raven (1997), it is evident that P_{max}, P_k ($\approx \alpha I$, under the assumption that I is subsaturating), and a^* can all depend on n:

$$P_{max}^* = \frac{n}{\tau}, \tag{11}$$

$$\alpha^* = n\sigma_{PSII}, \tag{12}$$

$$a^* = n\sigma_{PSU}, \tag{13}$$

where τ^{-1} is the rate at which electrons are transferred from H_2O to CO_2 at steady state (s^{-1}), σ_{PSII} is the cross section of photosystem II (m^2 mole quanta^{-1}), and σ_{PSU} is the cross section of the photosynthetic unit (m^2 mole PSU^{-1}). Assuming τ, σ_{PSII} and σ_{PSU} remain constant, a decrease in n with cell size will result in a corresponding decrease in a^*, P_k^C, and P_{max}^C. This decrease in n can also account for the strong correlation found between $\bar{a}^C$ and the photosynthetic parameters.

An organism's size is often a good predictor of its metabolic rate. For many different taxonomic groups, metabolic rate follows the $-1/4$ rule. This study confirms that the allometric power law is a good model for the prediction of light-limited, nutrient-saturated metabolic processes in marine diatoms. However, the $-1/4$ rule does not adequately describe the size dependence of light-limited anabolic rates, which appear to be influenced by the package effect. The integration of a bio-optical description of photosynthesis with the traditional allometric model provides a mechanism to understand the anomalous size scaling of metabolic rates in phytoplankton. Future work should focus on the role of light absorption and pigment packaging in the size scaling of metabolic rates in different taxonomic groups of phytoplankton, under a variety of growth conditions.

References

AGUSTI, S. 1991. Allometric scaling of light absorption and scattering by phytoplankton cells. Can. J. Fish. Aquat. Sci. **48:** 763–767.

BANSE, K. 1976. Rates of growth, respiration and photosynthesis of unicellular algae as related to cell size—a review. J. Phycol. **12:** 135–140.

BEUCHAT, C. 1997. Allometric scaling laws in biology. Science **278:** 371.

BLASCO, D., T. T. PACKARD, AND P. C. GARFIELD. 1982. Size dependence of growth rate, respiratory electron transport system activity, and chemical composition in marine diatoms in the laboratory. J. Phycol. **18:** 58–63.

CHISHOLM, S. W. 1992. Phytoplankton size, p. 213–237. *In* P. G. Falkowski and A. D. Woodhead [ed.]. Primary productivity and biogeochemical cycles in the sea. Plenum.

CULLEN, J. J., R. J. GEIDER, J. ISHIZAKA, D. A. KIEFER, J. MARRA, E. SAKSHAUG, AND J. A. RAVEN. 1993. Toward a general description of phytoplankton growth for biogeochemical models, p. 153–176. *In* G. T. Evans and M. J. R. Fasham [ed.]. Towards a model of ocean biogeochemical processes, v. I 10, NATO ASI series. Springer-Verlag.

FALKOWSKI, P. G. 1981. Light-shade adaptation and assimilation numbers. J. Plankton Res. **3:** 203–216.

———, AND J. RAVEN. 1997. Aquatic photosynthesis. Blackwell.

FINKEL, Z. V., AND A. J. IRWIN. 2000. Modeling size-dependent photosynthesis:light absorption and the allometric rule. J. Theor. Biol. **204:**: 61–369.

GEIDER, R. J., R. M. GREENE, Z. KOLBER, H. L. MACINTYRE, AND P. G. FALKOWSKI. 1993. Fluorescence assessment of the maximum quantum efficiency of photosynthesis in the western North Atlantic. Deep-Sea Res. **40:** 1205–1224.

———, AND B. A. OSBORNE. 1992. Algal photosynthesis. Chapman and Hall.

———, T. PLATT, AND J. A. RAVEN. 1986. Size dependence of growth and photosynthesis in diatoms: A synthesis. Mar. Ecol. Prog. Ser. **30:** 93–104.

GUILLARD, R. 1973. Division rates, p. 289–312. *In* J. Stein [ed.]. Handbook of phycological methods: Culture methods and growth measurements. Cambridge Univ. Press.

GUILLARD, R. R. L., AND J. H. RYTHER. 1962. Studies of marine planktonic diatoms. I. *Cyclotella nana* Hustedt and *Detonula confervacea* Cleve. Can. J. Microbiol. **8:** 229–239.

HEAD, E. J. H., AND E. P. W. HORNE. 1993. Pigment transformation and vertical flux in an area of convergence in the North Atlantic. Deep-Sea Res. II **40:** 329–346.

HEMMINGSEN, A. M. 1960. Energy metabolism as related to body size and respiratory surfaces, and its evolution. Rep. Steno Memorial Hosp. **9:** 15–22.

HOEPFFNER, N., AND S. SATHYENDRANATH. 1993. Determination of

the major groups of phytoplankton pigments from the absorption spectra of total particulate matter. J. Geophys. Res. **98:** 22,789–22,803.

HOLM-HANSEN, O., C. J. LORENZEN, R. W. HOLMES, AND J. D. H. STRICKLAND. 1965. Fluorometric determination of chlorophyll. J. Cons. Cons. Int. Explor. Mer **30:** 3–15.

IRWIN, B., C. CAVERHILL, P. DICKIE, E. HORNE, AND T. PLATT. 1986. Primary productivity on the Labrador Shelf during June and July 1984. Can. Data Rep. Fish. Aquat. Sci. **577.**

JOINT, I., AND A. POMROY. 1988. Allometric estimation of the productivity of phytoplankton assemblages. Mar. Ecol. Prog. Ser. **47:** 161–168.

KEPKAY, P. E., J. F. JELLETT, AND S. E. H. NIVEN. 1997. Respiration and the carbon-to-nitrogen ratio of a phytoplankton bloom. Mar. Ecol. Prog. Ser. **150:** 249–261.

KERMACK, K. A., AND J. HALDANE. 1950. Organic correlation and allometry. Biometrika **37:** 30–41.

KIØRBOE, T. 1993. Turbulence, phytoplankton cell size, and the structure of pelagic food webs. Adv. Mar. Biol. **29:** 1–72.

KIRK, J. T. O. 1994. Light and photosynthesis in aquatic ecosystems, 2nd ed. Cambridge Univ. Press.

KLEIBER, M. 1961. The fire of life: an introduction to animal energetics. John Wiley & Sons.

KYEWALYANGA, M. 1997. Spectral-dependence of photosynthesis in marine phytoplankton. Ph.D. thesis, Dalhousie University.

LABARBERA, M. 1989. Analyzing body size as a factor in ecology and evolution. Ann. Rev. Ecol. Systems **20:** 97–117.

LEVY, E. M., C. C. CUNNINGHAM, C. D. W. CONRAD, AND J. D. MOFFATT. 1977. The determination of dissolved oxygen in seawater. Bedford Inst. Oceanogr. Rep. Ser. **BI-R-77-9:** 16.

LEWIS, W. M., JR. 1989. Further evidence for anomalous size scaling of respiration in phytoplankton. J. Phycol. **25:** 395–397.

LI, W. K. W. AND J. C. GOLDMAN. 1981. Problems in estimating growth rates of marine phytoplankton from short-term ^{14}C assays. Microb. Ecol. **7:** 13–121.

MCMAHON, T. A. 1973. Size and shape in biology. Science **179:** 1201–1204.

MITCHELL, B. G. 1990. Algorithms for determining the absorption coefficient of aquatic particulates using the quantitative filter technique (QFT). Proceedings of the Society of Photo-Optical Instrumentation Engineers. Ocean Optics X. **1302:** 137–148.

MOREL, A., AND A. BRICAUD. 1981. Theoretical results concerning light absorption in a discrete medium, and application to specific absorption of phytoplankton. Deep-Sea Res. I **28A:** 1375–1393.

———, AND ———. 1986. Inherent optical properties of algal cells including picoplankton: theoretical and experimental results. *In* T. Platt and W. K. W Li [eds.]. Photosynthetic picoplankton. Can. Bull. Fish. Aquat. Sci. **214:** 521–558.

PETERS, R. H. 1983. The ecological implications of body size. Cambridge Univ. Press.

PLATT, T., AND A. D. JASSBY. 1976. The relationship between photosynthesis and light for natural assemblages of coastal marine phytoplankton. J. Phycol. **12:** 421–430.

RICKER, W. E. 1973. Linear regressions in fisheries research. J. Fish. Res. Board Can. **30:** 409–434.

ROUND, F. E., R. M. CRAWFORD, AND D. G. MANN. 1990. The Diatoms: Biology and morphology of the genera. Cambridge Univ. Press.

SCHLESINGER, D. A., L. A. MOLOT, AND B. G. SHUTER. 1981. Specific growth rates of freshwater algae in relation to cell size and light intensity. Can. J. Fish. Aquat. Sci. **38:** 1052–1058.

SOMMER, U. 1989. Maximal growth rates of Antarctic phytoplankton: Only weak dependence on cell size. Limnol. Oceanogr. **34:** 1109–1112.

SOSIK, H. M., AND B. G. MITCHELL. 1991. Absorption, fluorescence, and quantum yield for growth in nitrogen-limited *Dunaliella tertiolecta.* Limnol. Oceanogr. **36:** 910–921.

SUKENIK, A., J. BENNETT, A. MORTAIN-BERTRAND, AND P. G. FALKOWSKI. 1990. Adaptation of the photosynthetic apparatus to irradiance in *Dunaliella tertiolecta.* Plant Physiol. **92:** 891–898.

TAGUCHI, S. 1976. Relationship between photosynthesis and cell size of marine diatoms. J. Phycol. **12:** 185–189.

TANG, E. P. Y. 1995. The allometry of algal growth rates. J. Plankton Res. **17:** 1325–1335.

TANG, E. P. Y., AND R. H. PETERS. 1995. The allometry of algal respiration. J. Plankton Res. **17:** 303–315.

UKELES, R. 1973. Continuous culture—a method for the production of unicellular algal foods, p. 233–254. *In* J. Stein [ed.]. Handbook of phycological methods: culture methods and growth measurements. Cambridge Univ. Press.

WEST, G. B., J. H. BROWN, AND B. J. ENQUIST. 1997. A general model for the origin of allometric scaling laws in biology. Science **276:** 122.

YORK, D. 1966. Least-squares fitting of a straight line. Can. J. Phys. **44:** 1079–1086.

Received: 12 October 1999
Accepted: 10 July 2000
Amended: 18 September 2000